ELSEVIER

SCIENCE DIRECT

Physics Letters B 597 (2004) 263–269

PHYSICS LETTERS B

www.elsevier.com/locate/physletb

Discovery of a strange tribaryon $S^0(3115)$ in ^{4}He(stopped K^-, p) reaction

T. Suzuki [a], H. Bhang [b], G. Franklin [c], K. Gomikawa [a], R.S. Hayano [a], T. Hayashi [d,1], K. Ishikawa [d], S. Ishimoto [e], K. Itahashi [f], M. Iwasaki [f,d], T. Katayama [d], Y. Kondo [d], Y. Matsuda [f], T. Nakamura [d], S. Okada [d,2], H. Outa [e,2], B. Quinn [c], M. Sato [d], M. Shindo [a], H. So [b], P. Strasser [f,3], T. Sugimoto [d], K. Suzuki [a,4], S. Suzuki [e], D. Tomono [d], A.M. Vinodkumar [d], E. Widmann [a], T. Yamazaki [f], T. Yoneyama [d]

[a] *Department of Physics, University of Tokyo, Hongo, Bunkyo-ku, Tokyo 113-0033, Japan*
[b] *Department of Physics, Seoul National University, Shikkim-dong, Kwanak-gu, Seoul 151-742, South Korea*
[c] *Department of Physics, Carnegie Mellon University, Pittsburgh, PA 15213, USA*
[d] *Department of Physics, Tokyo Institute of Technology, Ookayama, Meguro-ku, Tokyo 152-8551, Japan*
[e] *IPNS, KEK (High Energy Acceralator Research Organization), Oho, Tsukuba-shi, Ibaraki 305-0801, Japan*
[f] *DRI, RIKEN, Wako-shi, Saitama 351-0198, Japan*

Received 1 June 2004; received in revised form 2 July 2004; accepted 23 July 2004

Available online 30 July 2004

Editor: J.P. Schiffer

Abstract

We have measured the proton energy distribution from the ^{4}He(stopped K^-, p) reaction by means of time-of-flight. A mono-energetic peak was observed, which is interpreted as the formation of a new kind of neutral tribaryon $S^0(3115)$ with isospin $T = 1$ and strangeness $S = -1$. The mass and width of the state were deduced to be $3117.0^{+1.5}_{-4.4}$ MeV/c^2 and < 21 MeV/c^2, respectively. The state mainly decays into ΣNN.

E-mail address: takatosi@nucl.phys.s.u-tokyo.ac.jp (T. Suzuki).
[1] Present address: Department of Legal Medicine, Osaka University.
[2] Present address: DRI, RIKEN.
[3] Present address: IMSS, KEK.
[4] Present address: Physik-Department E12, Technische Universität München.

0370-2693
doi:10.1016/j.physletb.2004.07.046

1. Introduction

Recently, the existence of deeply bound $\bar{K}$-nuclear systems has been predicted. In particular, based on an assumption of $\Lambda(1405)$ being an isospin $T = 0$ $\bar{K}N$ bound state, Akaishi and Yamazaki [1] constructed a bare $\bar{K}N$ potential so as to simultaneously reproduce the $\bar{K}N$ scattering lengths [2], the binding energy and width of the kaonic hydrogen atom [3] and those of $\Lambda(1405)$. They then used the g-matrix method to study the structure of $\bar{K}$ nuclear systems in light nuclei, and predicted discrete $\bar{K}$-bound states with large binding energies, narrow widths and high nucleon densities. For example, the nuclear ground state of a K^- in ^{3}He is predicted to be $T = 0$ with a binding energy of 108 MeV and a total width of 32 MeV. The narrow width results from the closing of the main decay channels to $\Sigma\pi NN$. Such deeply bound states have not been seen so far, and definitive experiments have been awaited.

We therefore used the ^{4}He(stopped K^-, n) reaction to search for the predicted deeply bound $(\bar{K}NNN)^{Z=1}_{T=0}$ state. If the deeply bound kaonic nuclear states exist, they will be formed via

$$\left(K^- {}^4\mathrm{He}\right)_{\mathrm{atomic}} \to \left(\bar{K}NNN\right)^{Z=1}_{T=0} + n,$$

and appear as distinct peaks in the emitted neutron energy spectrum [1,4]. The $(\bar{K}NNN)^{Z=1}_{T=0}$ is expected to decay strongly into $\Lambda\pi NN$, ΣNN, or ΛNN, and hence secondary charged particles $\pi^\pm$ or p should appear in the final state. We measured the neutron energy spectrum by means of time of flight (TOF), in coincidence with incident kaons and secondary charged particles from this reaction [5].

We also measured a proton energy spectrum in ^{4}He(stopped K^-, p) ($T = 1$ formation channel), in which no peak was predicted to appear. Quite unexpectedly, we observed a distinct peak with an overwhelming statistical significance. In this Letter, we present this surprising result.

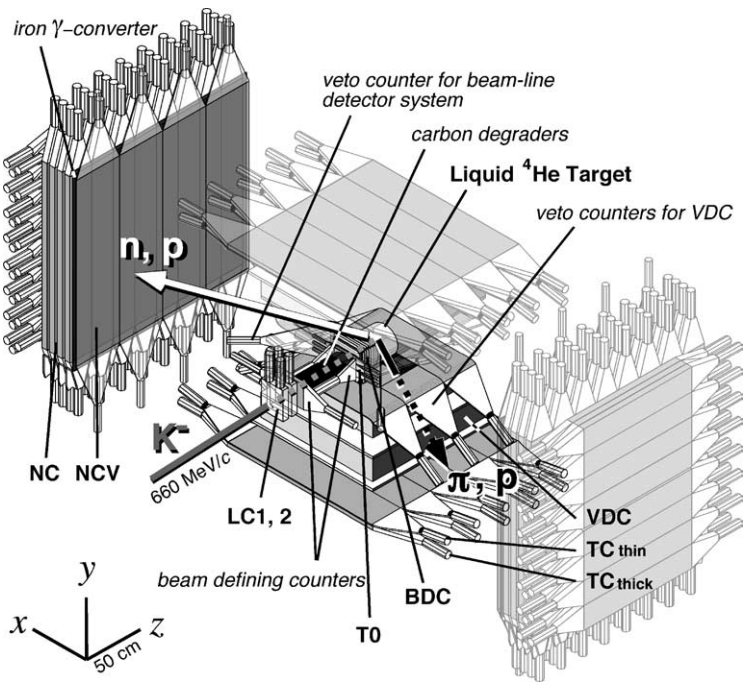

Fig. 1. An overview of the experimental setup. LC1, 2: Lucite Cherenkov counters, T0: beam timing counter, BDC: beamline drift chamber, VDC: vertex drift chamber, TC_{thin} and TC_{thick}: thin (0.6 cm) and thick (3 cm) trigger counter, NCV: neutron-counter charged-particle veto, NC: neutron-counter wall.

2. The experiment

Experiment E471 was performed at the K5 beamline at the KEK 12 GeV proton synchrotron. An overview of the experimental setup is shown in Fig. 1, together with the coordinate system we use throughout this Letter. In this experiment, we stopped negative kaons in a liquid helium target, and measured the TOF of neutrons/protons, detected by the neutron-counter (NC) walls. The possible fake structure in TOF spectra, originated from micro-structure of the beam, can be safely excluded. In fact, the time-structure of the beam is fairly flat except for weak modulation with a 10^{-3} second time scale, and no structure was found in the beam-monitoring time spectra with a 10^{-8}–10^{-9} second time scale. The TOF was obtained from the time difference between kaon arrival (defined by the counter T0) and neutron/proton hit on NC, corrected for the 'kaon stopping time' (the time elapsed since the kaon penetrated T0 until it is stopped in the target). The 'kaon stopping time' was inferred from the kaon reaction vertex position, namely, the crossing point of the kaon track, measured with beamline drift chambers (BDC), and a secondary charged particle track measured with vertex drift chambers (VDC). The correlation between the energy loss in the T0 counter and the vertex z position was used to reject in-flight reactions. A detailed description of the apparatus is given in Ref. [4]. We discuss some features essential to the present measurement in the following.

The target was superfluid helium (15 cm long and 23.5 cm in diameter) at a density of 0.145 g/cm^3. The target cell was made of a 0.6-mm-thick aluminum cylinder with thin-Mylar-film windows, surrounded by a 0.2-mm-thick aluminum heat-shield and a 0.9-mm-thick CFRP (carbon fiber reinforced plastic) vacuum vessel, so as to minimize the amount of material.

Neutron-counter walls (NC), each consisting of seven layers of segmented plastic scintillators covering an area of 1.5 m (in y) $\times$ 1.6 m (in z), were installed with their front faces positioned at $x = \pm 2$ m from the center of the target. Just in front of each NC, charged-particle veto counters (NCV) were placed. In between the NCV and the NC, a 4.5-mm-thick iron plate was inserted. For the proton measurement, only the inner-most NC layers were used for TOF measurement, and layers behind were used as calorimeters. As each NC segment was viewed by two photomultiplier tubes, the vertical (y) position of the NC hit point was obtained from the top–bottom time difference. The gamma-ray conversion events occurring in the iron plate were used for the absolute calibration of the TOF offset. This was essential to assure reliable TOF measurement, but in the case of proton detection, it introduced a momentum cutoff around 340–350 MeV/c (corresponding to the average material thickness of 4.1 g/cm^2, to which the iron plate contributed 3.5 g/cm^2).

The secondary charged particles emitted from the reaction point were detected by vertex detectors, positioned just above and below the target to cover a total solid angle of $\approx 40\%$ seen from the target center. Each set consisted of drift chambers (VDC) and a thin (0.6 cm thick) and a thick (3.0 cm thick) plastic scintillation counter (TC_{thin} and TC_{thick}, respectively).

The trigger condition required that we have a kaon (identified by the two sets of Cherenkov counters, LC1 and LC2), a hit in the NC, and a hit in the TC. The total number of events we accumulated corresponds to 2×10^8 stopped kaons.

3. Detector performance

The proton inverse velocity ($1/\beta$) and hence its momentum were calculated from its TOF and flight distance, the distance between the reaction vertex and the hit point on the NC. By using the gamma-conversion events, we calibrated the TOF offset, so that $1/\beta$ for gamma rays peaked at 1. This peak was broadened due to delayed gamma rays, which mainly came from $\Lambda \to n\pi^0$ decay followed by $\pi^0 \to 2\gamma$. The reaction vertex deduced as discussed above does not necessarily correspond to the gamma-emission point in this case. The $1/\beta$ resolution for gamma-ray events thus obtained is 0.046, while the convolution of resolutions of individual detectors and kaon-stopping-time correction gives a resolution of 0.030. We take the latter value to be the lower limit of the instrumental resolution.

Charged particles were selected by requiring a hit in the NCV counter in front of the NC. From the correlation between $1/\beta$ determined by the first layer and the total light output on NC, protons were clearly selected as shown in Fig. 2. When the selected proton

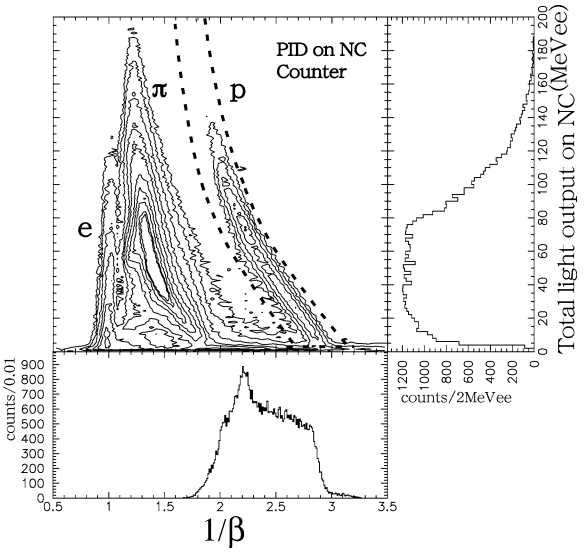

Fig. 2. Proton identification using the NC detector. It is performed by using a 2-dimensional correlation shown. The ordinate is the total NC light output in the unit of MeVee (MeV electron equivalent), and the abscissa is $1/\beta$. We see $e^{\pm}$ around $1/\beta = 1$, and a dominant band due to $\pi^{\pm}$ between $1/\beta \approx 1.2$ and 2.0. Projections of the proton events (surrounded by the dotted lines) onto each axis are also insetted.

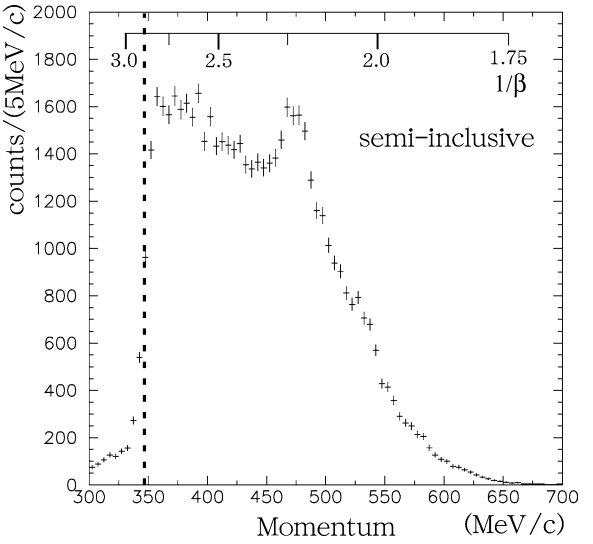

Fig. 3. Semi-inclusive proton momentum spectrum without energy-loss correction, showing a peak just below 500 MeV/c.

events are projected onto each axis, a large peak appears around $1/\beta \approx 2.2$.

4. Proton momentum spectrum and its classification

We obtained the proton momentum spectrum from the TOF and the flight distance, with the identification discussed in the previous section, as shown in Fig. 3. Note that this is a semi-inclusive spectrum, since the trigger condition required the detection of a secondary charged particle in TC. Also note that the proton energy-loss correction in the target, which amounts to ≈ 30 MeV/c at 500 MeV/c, is not yet applied at this stage. A significant peak exists just below 500 MeV/c, on a broad continuum which extends to ~ 700 MeV/c. As noted above, the sharp cutoff around 340–350 MeV/c, which is shown by a vertical dashed line in Fig. 3, is caused by the iron plate inserted between the NCV and NC counters.

The continuum protons in the momentum region between 340 MeV/c and 700 MeV/c originate mainly from non-mesonic K^- absorption, namely, $K^- \tilde{N}\tilde{N} \to YN$ or $K^- \tilde{N}\tilde{N}\tilde{N} \to YNN$, where N and Y denote nucleons (p, n) and hyperons $(\Lambda, \Sigma^0, \Sigma^{\pm})$, respectively, and $\tilde{N}$ denotes bound nucleons in the ^{4}He nucleus. Protons from successive hyperon decays $Y \to p\pi$ also contribute to the continuum. None of these can produce a discrete proton peak at around 500 MeV/c.

The nature of the observed peak can be investigated using the pulse-heights of TC counters as follows. In Fig. 4, we show a correlation between the light output on TC_{thin} and that on TC_{thick}. In about 90% of all events, a charged particle penetrated TC_{thin} and reached TC_{thick}. The correlation exhibits two bands, one due to protons, and the other due to $\pi^{\pm}$. As it is seen in the figure, both pion and proton distributions double back at the momentum where these particles start penetrating the TC_{thick} counter (~ 90 MeV/c for pion). Stopped π^- cause nuclear reaction on TC_{thick}, and the light output distribution on it has a large tail structure for pion, while the phenomenon is not expected for stopped proton. Thus, the correlation for the proton is a clear wedge-like structure, whereas it gets blurred for pions. Therefore, we defined a proton cut ("p"-cut) and a pion cut ("π"-cut) as indicated by the dashed lines in Fig. 4.

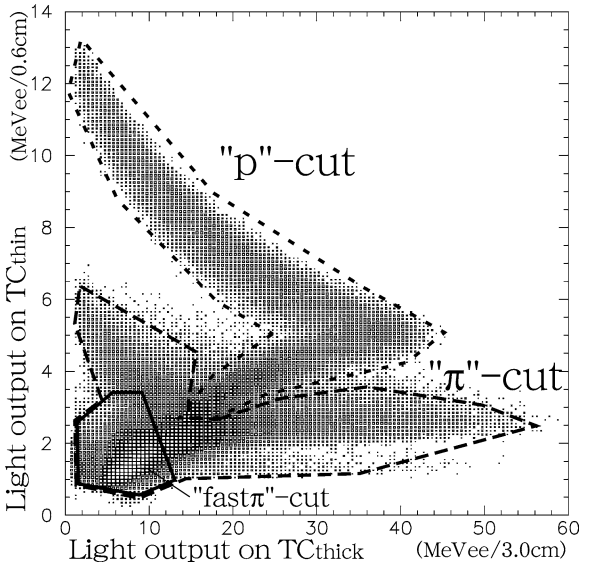

Fig. 4. Discrimination of relatively fast secondary charged particles with the trigger counters (TC). The ordinate and the abscissa are the detected light output per detector thickness on TC_{thin} and TC_{thick} in MeVee units, respectively.

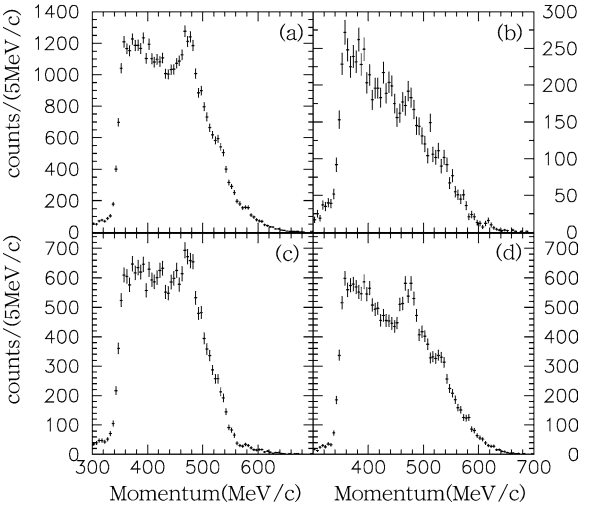

Fig. 5. Proton momentum spectra without energy-loss correction, with cut conditions defined in Fig. 4: (a) with the "π"-cut, (b) with the "p"-cut, (c) with "fast-π"-cut, and (d) with "π"-cut excluding the fast pions.

In the top panels of Fig. 5, we show two momentum spectra (still without energy-loss correction), where (a) is with the "π"-cut and (b) is with the "p"-cut. As shown, the peak is significant only when the secondary particle is a pion. This can be understood in view of possible decay modes of the observed state, as will be discussed later. Let us now show that the discrete peak is evidence for the formation of a hitherto unknown object via the ^{4}He(stopped K^-, p) reaction. The only other process which can create a peak around 500 MeV/c is hypernuclear formation $K^- + {}^4\mathrm{He} \to {}^4_\Lambda\mathrm{He} + \pi^-$ followed by its decay ${}^4_\Lambda\mathrm{He} \to {}^3\mathrm{H} + p$. In this chain of processes, a 255 MeV/c pion from the kaon stopping point and a 508 MeV/c proton would be emitted, although the formation probability of this mono-energetic proton is expected to be at most 2×10^{-4} per stopped K^- [6]. This reaction chain being the source of the proton peak can be ruled out as follows. These 255 MeV/c pions should appear in connection with the region marked as "fast π" in Fig. 4 (a Monte Carlo simulation was used to define the "fast π" cut, so as to accept about 90% of the 255 MeV/c π^-). Fig. 5(c) was produced by selecting fast pions, while Fig. 5(d) by selecting remaining pions. If the peak originates from the hypernuclear decay, then 90% of the signal is expected to be in Fig. 5(c). However, the fact that the peak structure is as strong, or even stronger in Fig. 5(d) compared with (c), shows that the observed proton peak is not due to the hypernuclear non-mesonic decay.

5. Mass and decay modes

Let us call the object we found a strange tribaryon, S^0, and obtain its mass and width. Since the energy loss of the protons inside the target system is not negligible, we now apply an event-by-event correction for the proton energy loss, based on the proton TOF, reaction point, and detection point, then construct the missing mass spectrum.

Fig. 6 shows the resulting semi-inclusive missing mass spectrum. We fitted a Gaussian peak plus a second-order polynomial background to the 17 data points in the peak region as indicated in the figure. The fit χ^2 is 11.7 for 11 degrees of freedom and the statistical significance of the peak is 13 σ. The significance is defined as the signal area divided by its fit error, and includes the uncertainty of the background.

The fitted mass is $3117.0 \pm 0.7(\mathrm{stat})$ MeV/c^2, while our estimate for the systematic uncertainty in the absolute mass is $^{+0.8}_{-3.7}$ MeV/c^2. The fitted Gaussian

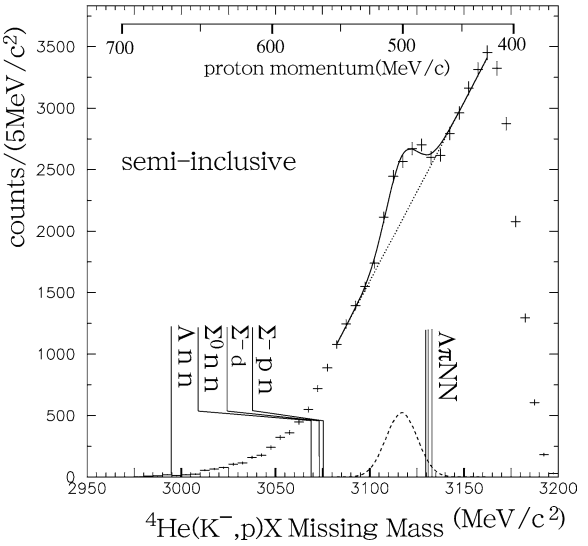

Fig. 6. Missing mass spectrum of the semi-inclusive proton events with the proton momentum scale. The solid curve shows the best-fit to the spectrum with a Gaussian peak and a second-order polynomial background. The dashed line shows the Gaussian peak and the dotted line is the background. Possible decay modes are also shown at the corresponding mass thresholds.

width is $8.3 \pm 0.6(\text{stat}) \pm 1.1(\text{sys})$ MeV/c^2. The upper- and lower-limit of the $1/\beta$ resolution, 0.046 and 0.030 respectively, correspond to a mass resolution of 7.2 and 5.2 MeV/c^2 in the region of interest. Since the fitted width is close to the upper limit of the estimated instrumental resolution, the use of a Gaussian as the fit function is justified. Using the lower limit of the instrumental resolution, the natural width Γ_{S^0} is evaluated to be smaller than 21 MeV/c^2 at 95% confidence level.

In Fig. 6, possible decay modes and their thresholds are shown. The mesonic-decay mode, $\Lambda\pi NN$, is likely to be closed in view of the mass and width of $S^0(3115)$. This leaves us with the four non-mesonic modes, namely, Λnn, $\Sigma^0 nn$, $\Sigma^- np$ and $\Sigma^- d$, where the decay Q values for Λnn and ΣNN are ≈ 120 MeV and ≈ 50 MeV, respectively. According to Monte Carlo simulations, the large Q value of the Λnn decay implies that the proton from the $\Lambda \to p\pi^-$ is energetic enough to reach the TC counters, while at most 15% of the protons from Σ decays are expected to reach TC_{thin}. The fact that the $S^0(3115)$ peak is not pronounced in the "p"-cut spectrum (Fig. 5(b)) seems to exclude the Λnn being the dominant decay mode, and suggests that the main decay mode of $S^0(3115)$ is ΣNN.

The $S^0(3115)$ formation branching ratio per stopped K^- is estimated to be about 1%. Uncertainties of the S^0 decay modes and their branching ratios, and background physics processes (mainly due to K^- non-mesonic absorption as mentioned before) prevent us from deducing it more accurately at the moment.

6. Discussion and conclusions

The discrete proton peak observed in the stopped K^- reaction is evidence for the existence of charge 0, strangeness -1, baryon number 3 system, which we denote as $S^0(3115)$. Isospin conservation requires that the isospin of $S^0(3115)$ is $T = 1$. Assigning this narrow state to an excited state of a Λ hypernucleus (excitation energy ≈ 120 MeV) or a Σ hypernucleus (excitation energy ≈ 50 MeV) would be unconceivable. On the other hand, $S^0(3115)$ is different from what was originally predicted in Ref. [1], since it is neutral and $|T, T_z\rangle = |1, -1\rangle$. If this is a deeply-bound kaonic state, it must be $(\bar{K}NNN)^{Z=0}_{|T,T_z\rangle=|1,-1\rangle}$. Very recently, the possible existence of a deeply bound kaonic state $(\bar{K}NNN)^{Z=2}_{|T,T_z\rangle=|1,+1\rangle}$ has been predicted [7]. From that standpoint, $S^0(3115)$ may be interpreted as its isobaric analog state $(\bar{K}NNN)^{Z=0}_{|T,T_z\rangle=|1,-1\rangle}$ with a total binding energy of 194 MeV (measured from $K^- + p + n + n$ rest mass) [8]. However, $S^0(3115)$ is about 100 MeV/c^2 lighter than the predicted mass of $(\bar{K}NNN)^{Z=2}_{|T,T_z\rangle=|1,+1\rangle}$, and hence it is premature to judge whether or not $S^0(3115)$ fits within this framework.

We conclude that a new kind of neutral strange tribaryon, $S^0(3115)$, with a mass $3117.0^{+1.5}_{-4.4}$ MeV/c^2 and a width less than 21 MeV/c^2 (95% CL) has been discovered. Its main decay mode is consistent with ΣNN. The formation probability per stopped K^- is about 1%. So far, it is not clear whether this state can be understood in a hadronic picture like a deeply bound $(\bar{K}NNN)^{Z=0}_{|T,T_z\rangle=|1,-1\rangle}$ state, or would require a quark level description.

Acknowledgements

We are grateful to Y. Akaishi and R. Seki for useful discussion. We owe much to M. Iwai, T. Taniguchi,

O. Sasaki, M. Sekimoto and all the KEK staff members for their substantial cooperation. We thank IHI Co. Ltd. for collaborative development for the CFRP vacuum jacket. This work is supported by MEXT, KEK, RIKEN, KOSEF, NSF, DOE and KRF.

References

[1] Y. Akaishi, T. Yamazaki, Phys. Rev. C 65 (2002) 044005.
[2] A.D. Martin, Nucl. Phys. B 179 (1981) 33.
[3] M. Iwasaki, et al., Phys. Rev. Lett. 78 (1997) 3067;
T.M. Ito, et al., Phys. Rev. C 58 (1998) 2366.
[4] M. Iwasaki, et al., Nucl. Instrum. Methods Phys. Res. A 473 (2001) 286.
[5] M. Iwasaki, et al., nucl-ex/0310018, Phys. Lett. B, submitted for publication;
T. Suzuki, et al., Nucl. Phys. A, submitted for publication.
[6] H. Outa, et al., Nucl. Phys. A 639 (1998) 251c.
[7] T. Yamazaki, Y. Akaishi, Phys. Lett. B 535 (2002) 70;
T. Yamazaki, A. Dote, Y. Akaishi, Phys. Lett. B 587 (2004) 167;
A. Dote, H. Horiuchi, Y. Akaishi, T. Yamazaki, Phys. Lett. B 590 (2004) 51;
A. Dote, H. Horiuchi, Y. Akaishi, T. Yamazaki, nucl-th/0309062, Phys. Rev. C, in press.
[8] Y. Akaishi, private communication.